01 Jan 2018

Limit Analysis On Seismic Stability Of Anisotropic And Nonhomogeneous Slopes With Anti-slide Piles

Wei Bing Gong
Missouri University of Science and Technology, weibing.gong@mst.edu

Jing Pei Li

Lin Li

Recommended Citation

W. B. Gong et al., "Limit Analysis On Seismic Stability Of Anisotropic And Nonhomogeneous Slopes With Anti-slide Piles," *Science China Technological Sciences*, vol. 61, no. 1, pp. 140 - 146, Springer; Science China Press; Chinese Academy of Sciences; National Natural Science Foundation of China, Jan 2018.
The definitive version is available at https://doi.org/10.1007/s11431-017-9147-8

SCIENCE CHINA
Technological Sciences

• Article •

January 2018 Vol.61 No.1: 140–146
https://doi.org/10.1007/s11431-017-9147-8

Limit analysis on seismic stability of anisotropic and nonhomogeneous slopes with anti-slide piles

GONG WeiBing, LI JingPei* & LI Lin

[1] *Department of Geotechnical Engineering, Tongji University, Shanghai 200092, China;*
[2] *Key Laboratory of Geotechnical and Underground Engineering of Ministry of Education, Tongji University, Shanghai 200092, China*

Received March 29, 2017; accepted September 11, 2017; published online October 17, 2017

This study employs the limit analysis method to evaluate the seismic stability of anisotropic and nonhomogeneous slopes stabilized with anti-slide piles. The pseudo-static approach is used to simplify the earthquake load. The yield seismic acceleration factor is obtained from the optimization procedure and the results are verified with the published data. Then, the seismically-unstable slope is reinforced with anti-slide piles, and the seismic stability of the reinforced slope is explored. The results show that the anisotropy and nonhomogeneity of soils have significant effects on the stabilizing force required from the anti-slide piles and the optimal location of the pile is near the toe of the slope.

limit analysis, pseudo-static approach, anti-slide pile, optimal location

Citation: Gong W B, Li J P, Li L. Limit analysis on seismic stability of anisotropic and nonhomogeneous slopes with anti-slide piles. Sci China Tech Sci, 2018, 61: 140–146, https://doi.org/10.1007/s11431-017-9147-8

1 Introduction

Slopes can lose stability during earthquakes. Unstable slopes are usually stabilized by either reducing the driving force for failure (e.g. flattening slopes) or increasing the resisting force against failure (e.g. installing piles or retaining walls). Anti-slide piles are found effective for stabilizing slopes under static conditions [1–6]. However, to the best of authors' knowledge, the effectiveness of anti-slide piles for stabilizing seismic slopes remains unclear. Moreover, owning to the effects of consolidation pressures, stress history, cementation bonds and overconsolidation, natural soils exhibit remarkable anisotropy [7–9] and unneglectable nonhomogeneity [10]. Therefore, it seems more appropriate to incorporate the anisotropy and nonhomogeneity into the analysis of the stability of slopes with anti-slide piles.

The methods for analyzing the stability of slopes mainly fall into three categories: (1) the limit equilibrium method; (2) the numerical analysis method and (3) the limit analysis method. All these methods are useful for assessing the effect of seismic loads though with various degrees of approximation. The limit equilibrium method has been the dominant approach used for examining slope stability over the past several decades [11]. This method can be used for a variety of conditions, such as loading and seepage, without requiring additional computational efforts. However, owning to its arbitrary assumptions, the results produced by this method can represent neither the lower bound nor the upper bound of the true solution. Alternatively, the numerical approach such as the finite element method is considered, to some extent, as the most comprehensive means at present, because it allows for rather complex conditions and keeping track of progressive slope failures. However, the demand of high computational cost and intensive effort required for model calibration largely restricts its wide application and makes it less attractive in the routine practice of geotechnical engineering.

*Corresponding author (email: lijp2773@163.com)

The limit analysis method, based on the plasticity limit theorems, can provide rigorous lower and upper bounds that bracket the true solution. Although the kinematic method of the limit analysis is an approximate approach, the results obtained from reasonably assumed failure mechanisms have been proven credible [10]. Furthermore, the limit analysis method is much simpler to use under certain assumptions than the limit equilibrium method [1]. Recently, the limit analysis method is still popularly adopted to analyze slope stability. For example, Zhao et al. [12] explored the safety factors of homogeneous slopes under a general nonlinear failure criterion, where three shear strength reduction strategies were adopted; Tang et al. [13] developed stability charts of slopes under horizontal seismic force, surcharge load and pore water pressure in order to help geotechnical engineers quickly determine slope safety factors; Yang and Xu [14] investigated the influence of soil nonhomogeneity on the static and seismic three-dimensional stability of two-stage slopes; Subsequently, they [15] extended their nonhomogeneous solutions to nonhomogeneous and anisotropic solutions to explore the effects of either pore water pressure or seismic force on the stability of three-dimensional slopes. The above mentioned literature substantiates that the limit analysis is a vary effective method for analyzing slope stability. Hence, this method is also adopted in this study to investigate the seismic stability of anisotropic and nonhomogeneous slopes with anti-slide piles. The stability factor of anisotropic and nonhomogeneous slopes is first developed under the static condition, and then extended to the seismic condition. The effect and optimal location of anti-slide piles are finally studied to reach a desired level of seismic stability. Since it is prohibitive to consider every detail of earthquake loading in analytical analyses, the pseudo-static method is used. This method simplifies the earthquake-induced inertial force as the equivalent concentrated force acting on the center of gravity of the sliding soil mass. While this simplification has drawn some criticisms, it is widely accepted in practice as an economic solution with adequate accuracy for the analysis of seismic stability of slopes [16–19].

2 Anisotropy and nonhomogeneity of natural soils

The Mohr-Coulomb's failure criterion, which describes the strength of soils with two parameters, i.e. the cohesion, c, and the internal friction angle, φ, is employed. The reported studies [3,10] show that the anisotropy and nonhomogeneity of cohesion are more prominent than those of the internal friction angle. Hence, a constant internal friction angle is assumed and only anisotropy and nonhomogeneity of cohesion are considered in this study.

The anisotropy of soils is reflected by the cohesion variation along the shearing direction (see Figure 1(a)), and the cohesion in any direction is expressed as [3,10]

$$c_\psi = c_\mathrm{h} + (c_\mathrm{v} - c_\mathrm{h})\cos^2\psi, \tag{1}$$

where c_h and c_v are the cohesions in the horizontal and vertical directions, respectively; and ψ is an angle at which the major stress is inclined to the vertical direction; assuming the anisotropic coefficient $k=c_\mathrm{h}/c_\mathrm{v}$, eq. (1) can be written as:

$$c_\psi = c_\mathrm{h}\left(1 - \frac{1-k}{k}\cos^2\psi\right). \tag{2}$$

For isotropic soil, k=1 (i.e. $c_\psi=c_\mathrm{h}=c_\mathrm{v}$).

Because of the nonhomogeneity of soils, the cohesion can be assumed to increase linearly with the depth (see Figure 1(b)) [10,20]. The notation n in the figure is the nonhomogeneous coefficient. Under the particular case with $n_0=n_1=n_2=1$, the soils are homogenous and the cohesion remains constant with respect to the depth.

3 Stability of slopes subjected to seismic loads

3.1 Limit analysis and objective function

The kinematic method of the limit analysis states that the rate of the work done by external loads must equal the dissipation rate of internal energy at the critical state of slope collapse. The external loads include the slope weight, the seismic load and the surcharge load. The internal energy includes the energy generated along the assumed failure surface and by the anti-slide piles. By equating the external work rate to the internal energy dissipation rate, the upper bound of the true solution can be obtained. In this study, the classical log-spiral failure mechanism (see Figure 2) is adopted and the log-spiral function is expressed as:

$$r = r_0\exp\left[(\theta-\theta_0)\tan\varphi\right]. \tag{3}$$

The definitions of the variable θ, θ_0 and r_0 are referred to Figure 2. From the geometric relation shown in Figure 2, the ratio of the slope height, H, to the length of OB, r_0, and the ratio of the length of AB, L, to the length of OB, r_0, can be

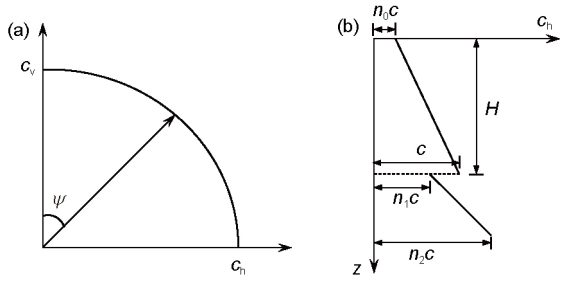

Figure 1 (a) Anisotropy of soils with direction; (b) nonhomogeneity of soils with depth.

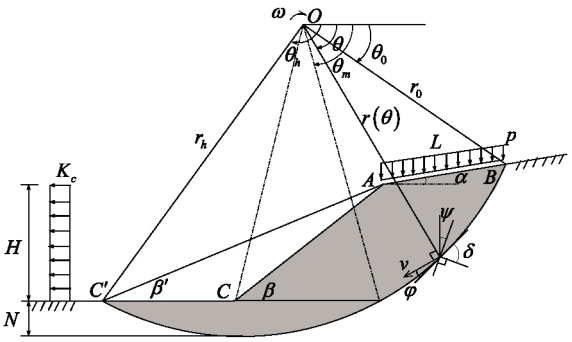

Figure 2 Log-spiral failure mechanism of slope under seismic and surcharge loads.

expressed, respectively, as:

$$\frac{H}{r_0}=\frac{\sin\beta'}{\sin(\beta'-\alpha)}\left\{-\sin(\theta_0+\alpha)+\sin(\theta_h+\alpha)\exp\left[(\theta_h-\theta_0)\tan\varphi\right]\right\}, \tag{4}$$

$$\frac{L}{r_0}=\frac{\sin(\theta_0+\beta')}{\sin(\beta'-\alpha)}-\exp\left[(\theta_h-\theta_0)\tan\varphi\right]\frac{\sin(\theta_h+\beta')}{\sin(\beta'-\alpha)}. \tag{5}$$

It is difficult to directly calculate the work rate by the weight of the moving mass represented by area $ACC'B$. Alternatively, it can be obtained by subtracting the work rate by the weight of mass represented by areas OAB, OAC' and $AC'C$ from that of mass of area OBC', i.e.

$$\dot{W}_{\text{ext}}^{G}=\gamma\omega r_0^3(f_1-f_2-f_3-f_4), \tag{6}$$

where γ is the unit weight of soil; ω is the angular velocity; and the expressions of the functions f_1, f_2, f_3 and f_4 can be found in the reference [10].

The rate of the internal energy dissipation taking place along the failure surface $C'B$ can be calculated as:

$$\dot{W}_{\text{int}}^{c}=\omega r_0^2\left\{\int_{\theta_0}^{\theta_m}c_{\psi 1}\exp\left[2(\theta-\theta_0)\tan\varphi\right]\mathrm{d}\theta+\int_{\theta_m}^{\theta_h}c_{\psi 2}\exp\left[2(\theta-\theta_0)\tan\varphi\right]\mathrm{d}\theta\right\}, \tag{7}$$

where the expressions of $c_{\psi 1}$ and $c_{\psi 2}$ are

$$c_{\psi 1}=c\left(1+\frac{1-k}{k}\cos^2\psi\right)\left[n_0+\frac{1-n_0}{H/r_0}\left\{\sin\theta\exp\left[(\theta-\theta_0)\tan\varphi\right]-\sin\theta_0\right\}\right], \tag{8}$$

$$c_{\psi 2}=c\left[\frac{n_2-n_1}{H/r_0}\left\{\sin\theta\exp\left[(\theta-\theta_0)\tan\varphi\right]-\sin\theta_m\exp\left[(\theta_m-\theta_0)\tan\varphi\right]\right\}+n_1\right]\left(1+\frac{1-k}{k}\cos^2\psi\right), \tag{9}$$

where θ_m can be determined by the following:

$$\sin\theta_h\exp(\theta_h\tan\varphi)=\sin\theta_m\exp(\theta_m\tan\varphi). \tag{10}$$

Note that the angle ψ can be obtained based on the following simple geometric relation shown in Figure 2:

$$\psi=\theta+\delta-\frac{\pi}{2}-\varphi=\theta+\Phi, \tag{11}$$

where $\delta=\pi/4+\varphi/2$ represents the angle between the tangential direction of the failure surface and the minor stress direction.

Equating eq. (6) to eq. (7) yields

$$r_0=\frac{c}{\gamma}\frac{f_c}{f_1-f_2-f_3-f_4}, \tag{12}$$

where the function f_c is the bracket part in eq. (7).

Assuming

$$f(\theta_0,\theta_h,\beta')=\frac{H}{r_0}\frac{f_c}{f_1-f_2-f_3-f_4}, \tag{13}$$

eq. (12) can be rewritten as:

$$H=\frac{c}{\gamma}f(\theta_0,\theta_h,\beta'). \tag{14}$$

The stability factor, N_s, is defined as the minimum value of the function $f(\theta_0, \theta_h, \beta')$, i.e. $N_s=\min f(\theta_0, \theta_h, \beta')$. However, due to the complexity of the implicit function eq. (13), it is difficult to directly find the stability factor, N_s. Alternatively, the optimization method is used to determine the stability factor by defining the objective function and the constraint conditions as follows:

$$\min f=f(\theta_0,\theta_h,\beta'),\ \text{s.t.}\begin{cases}0<\theta_0<\pi/2,\\ \theta_0<\theta_h<\pi,\\ 0<\beta'<\beta.\end{cases} \tag{15}$$

3.2 Pseudo-static analysis

As shown in Figure 2, the seismic load is replaced with an equivalent static distributed horizontal load pointing outward. Here, vertical shaking is not considered because it has little influence on slopes [19]. Although, this simplification is unable to reflect the true effect of the seismic action, it can provide a simple and useful tool to quantitatively assess the seismic stability of slopes. The value of the horizontal load is the product of the seismic acceleration factor, K, and the weight of the potential sliding soil mass. Hence, the work rate done by the seismic load can be calculated as

$$\dot{W}_{\text{ext}}^{S}=K\omega\gamma r_0^3(f_5-f_6-f_7-f_8), \tag{16}$$

in which the expressions of the functions f_5, f_6, f_7 and f_8 are

$$f_5=\frac{1}{3(1+9\tan^2\varphi)}\left\{\cos\theta_0-3\tan\varphi\sin\theta_0+(3\tan\varphi\sin\theta_h-\cos\theta_h)\exp\left[3(\theta_h-\theta_0)\tan\varphi\right]\right\}, \tag{17}$$

$$f_6 = \frac{1}{6}\frac{L}{r_0}\left(2\sin\theta_0 + \frac{L}{r_0}\sin\alpha\right)\sin(\theta_0+\alpha), \tag{18}$$

$$f_7 = \frac{1}{6}\left[\sin(\theta_h-\theta_0) - \frac{L}{r_0}\sin(\theta_h+\alpha)\right] \left\{\sin\theta_0 + \frac{L}{r_0}\sin\alpha + \sin\theta_h \exp\left[(\theta_h-\theta_0)\tan\varphi\right]\right\} \exp\left[(\theta_h-\theta_0)\tan\varphi\right], \tag{19}$$

$$f_8 = \frac{\sin(\beta-\beta')}{2\sin\beta\sin\beta'}\left(\frac{H}{r_0}\right)^2\left(\frac{2}{3}\frac{H}{r_0} + \sin\theta_0 + \frac{L\sin\alpha}{r_0}\right). \tag{20}$$

Similarly, the work rate done by the surcharge load can be calculated as:

$$\dot{W}_{\text{ext}}^{p} = p\omega r_0^2(f_v + xKf_h), \tag{21}$$

where the parameter x is the ratio of the seismic acceleration factor of the surcharge load to the seismic acceleration factor of the soil weight, and the value of x varies from 0 to 1. The functions f_v and f_h are given by

$$f_v = \frac{L}{r_0}\left(\cos\theta_0 - \frac{1}{2}\frac{L}{r_0}\cos\alpha\right), \tag{22}$$

$$f_h = \frac{L}{r_0}\left(\sin\theta_0 + \frac{1}{2}\frac{L}{r_0}\sin\alpha\right). \tag{23}$$

Equating the external work rate to the internal energy dissipation rate, and with the substitution of eq. (4), an upper bound value of the seismic acceleration factor can be obtained as:

$$K = \frac{cf_c - \gamma H/\overline{H}(f_1 - f_2 - f_3 - f_4) - pf_v}{\gamma H/\overline{H}(f_5 - f_6 - f_7 - f_8) + xpf_h}, \tag{24}$$

where the expression of $\overline{H}$ is

$$\overline{H} = \frac{\sin\beta'}{\sin(\beta'-\alpha)}\left\{-\sin(\theta_0+\alpha) + \sin(\theta_h+\alpha)\exp\left[(\theta_h-\theta_0)\tan\varphi\right]\right\}. \tag{25}$$

When eq. (24) reaches its minimum value, the yield seismic acceleration factor, K_c, is obtained, i.e. K_c=min $K(\theta_0, \theta_h, \beta')$.

3.3 Verifications

There are few documented studies on slope stability considering both anisotropy and nonhomogeneity of soils. The studies available to verify the proposed solution were presented by the literature [3,10]. In their studies, the cohesion increases linearly with depth and passes through the coordinate origin. Therefore, the values of the nonhomogeneous coefficients are n_0=0, n_1=1 and n_2=1+N/H (i.e. n=z/H). By substituting these nonhomogeneous coefficients into eqs. (8) and (9), the function f_c can be simply expressed as

$$f_c = \frac{1}{(H/r_0)\exp(3\theta_0\tan\varphi)} \left\{\zeta(\theta) - \xi(\theta)\sin\theta_0\exp(\theta_0\tan\varphi) + \frac{1-k}{k}\left[\Psi(\theta) - \Theta(\theta)\sin\theta_0\exp(\theta_0\tan\varphi)\right]\right\}_{\theta_0}^{\theta_h}, \tag{26}$$

where the expressions of the functions $\zeta(\theta)$, $\xi(\theta)$, $\Psi(\theta)$ and $\Theta(\theta)$ are as follows:

$$\xi(\theta) = \frac{\exp(2\theta\tan\varphi)}{2\tan\varphi}, \tag{27}$$

$$\zeta(\theta) = \frac{(3\tan\varphi\sin\theta - \cos\theta)\exp(3\theta\tan\varphi)}{1+9\tan^2\varphi}, \tag{28}$$

$$\Psi(\theta) = \frac{\exp(3\theta\tan\varphi)}{2}\left\{\cos 2\Phi\left[\frac{\cos\theta - 3\tan\varphi\sin\theta}{2(1+9\tan^2\varphi)} + \frac{\tan\varphi\sin 3\theta - \cos 3\theta}{6(1+\tan^2\varphi)}\right] - \left[\frac{\sin\theta + 3\tan\varphi\cos\theta}{2(1+9\tan^2\varphi)} - \frac{\tan\varphi\cos 3\theta + \sin 3\theta}{6(1+\tan^2\varphi)}\right]\sin 2\Phi - \frac{\cos\theta - 3\tan\varphi\sin\theta}{1+9\tan^2\varphi}\right\}, \tag{29}$$

$$\Theta(\theta) = \left\{\cos 2\Phi\left[\frac{\tan\varphi\cos 2\theta + \sin 2\theta}{2(1+\tan^2\varphi)}\right] - \sin 2\Phi\left[\frac{\tan\varphi\sin 2\theta - \cos 2\theta}{2(1+\tan^2\varphi)}\right]\right\}\frac{\exp(2\theta\tan\varphi)}{2} + \frac{\exp(2\theta\tan\varphi)}{4\tan\varphi}. \tag{30}$$

Substituting eq. (26) into eq. (13), the stability factor, N_s, that considers both the anisotropy and nonhomogeneity of soils, can be obtained by the optimization method. The calculated results and the published data are tabulated in Table 1. A good agreement is found between them.

In order to verify the present solution for slopes subjected to seismic loads, the results of the yield seismic acceleration factors are compared with those reported by the literature [16]. With the optimization method, the minimum values of eq. (24), i.e. the yield seismic acceleration factors, K_c, are obtained. The results without considering the anisotropy and nonhomogeneity of soils are summarized in Table 2. The comparison demonstrates a good agreement.

To further investigate the effects of anisotropy and nonhomogeneity of soils on the yield seismic acceleration factors, the calculated values of K_c considering only anisotropy and considering both anisotropy and nonhomogeneity (n=z/H) are shown in Figures 3 and 4, respectively. It is found that the anisotropy of soils has significant effects on K_c. The yield seismic acceleration factor decreases with the decrease of

Table 1 Comparison of stability factors N_s for anisotropic and nonhomogeneous slopes

	φ=10°, β=50°, α=0°			φ=30°, β=50°, α=0°		
	k=1	k=0.8	k=0.5	k=1	k=0.8	k=0.5
Chen [10]	5.44	5.26	4.95	15.50	14.96	14.09
Nian et al. [3]	5.44	5.27	4.96	15.51	14.98	14.11
Present study	5.44	5.26	4.95	15.45	14.90	14.06

Table 2 Comparison of the yield seismic acceleration factors K_c for isotropic and homogeneous slopes with H=30.48 m and α=0°

	p=5.75 kPa, x=0			p=5.75 kPa, x=0.5		
	β=45°	β=60°	β=75°	β=45°	β=60°	β=75°
Chang et al. [16]	0.677	0.513	0.324	0.671	0.506	0.320
Present study	0.678	0.513	0.325	0.671	0.506	0.320

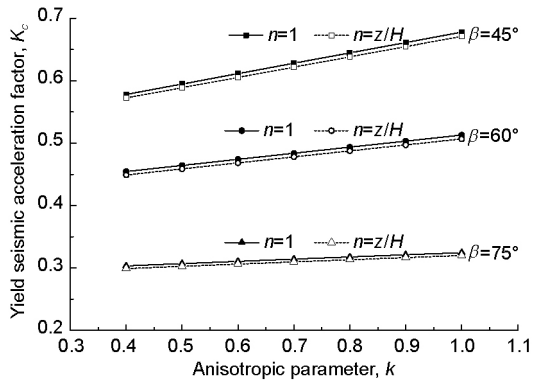

Figure 3 Effects of anisotropy and nonhomogeneity of soils on yield seismic acceleration factor, K_c, with p=5.75, x=0.

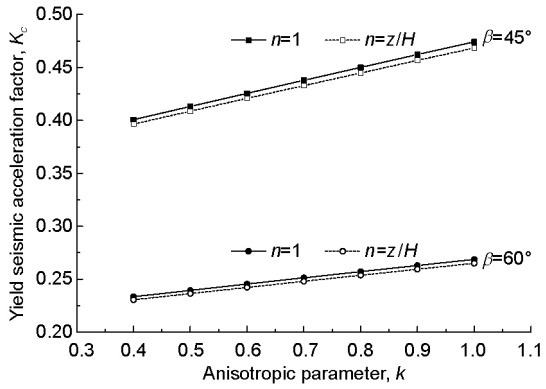

Figure 4 Effects of anisotropy and nonhomogeneity of soils on yield seismic acceleration factor, K_c, with p=5.75, x=0.5.

anisotropic coefficient. In other words, when soils show stronger anisotropy, the slope can only resist a weaker earthquake. Moreover, the yield seismic acceleration factor of gentle slopes decreases faster than that of steep slopes. This indicates that the anisotropy of soils has a stronger impact on the stability of gentler slopes subjected to seismic loads. From the figures, it is noted that the yield seismic acceleration factors of slopes considering both anisotropy and nonhomogeneity are less than those only considering anisotropy, but the difference between them is small. In Table 2, the difference between the results with x=0 and those with x=0.5 is small, but the difference between the results shown in Figures 3 and 4 is quite large. The yield seismic acceleration factors of slopes with inclined angle β=75° are not included in Figure 4. This is because the yield seismic acceleration factors of such slopes subjected to both seismic and surcharge loads are very small and even close to zero. However, the value of K_c of the isotropic and homogenous slope is 0.320. Hence, it can be concluded that neglecting the effects of anisotropy and nonhomogeneity of soils could largely overestimate the earthquake resistance of slopes. This conclusion further supports the necessity for considering the anisotropy and nonhomogeneity of soils when evaluating the seismic stability of slopes.

4 Stability of slopes reinforced by piles

4.1 Required stabilizing forces provided by piles and optimal location of piles

When the yield seismic acceleration factor of a slope is smaller than the actual seismic acceleration factor of possible earthquakes, the slope needs engineering reinforcement by, for instance, installing piles to increase the yield seismic acceleration factor to a desired value. Figure 5 illustrates a pile-stabilized slope. The reinforced effect of a row of piles on the slope can be equivalent to a lateral force and a moment applied at the potential sliding surface [1,3]. The lateral force can be assumed to act in the horizontal direction [1] or parallel to the tangent direction of the log-spiral surface [3]. From the literature [3], there is little difference between the lateral forces obtained from these two directions. Hence, a horizontal force is assumed to arise from the piles. Accordingly, the internal energy dissipation rate generated by the

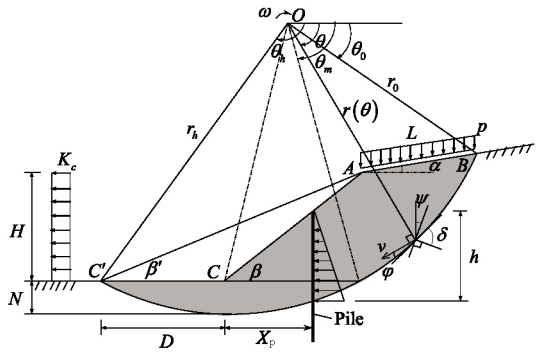

Figure 5 Log-spiral failure mechanism of pile-stabilized slope under seismic and surcharge loads.

piles can be obtained as:

$$W_{\text{int}}^{\text{p}}=F_{\text{p}}r_{\text{p}}\sin\theta_{\text{p}}\omega-F_{\text{p}}mh\omega, \tag{31}$$

where F_{p} is the stabilizing force provided by the piles; h is the height of the piles above the sliding surface; and m is a coefficient that represents the ratio of the height of F_{p} above the sliding surface to h. When the force is assumed to be linearly distributed between the ground surface and the sliding surface, m is equal to 1/3. The height, h, can be expressed in terms of the abscissa, X_{p}, measured from the slope toe as

$$\begin{aligned} &h=X_{\text{p}}\tan\beta+r_{\text{p}}\sin\theta_{\text{p}}-r_h\sin\theta_h,\\ &0\le X_{\text{p}}\le H\cot\beta, \end{aligned} \tag{32}$$

where X_{p}, is given by

$$X_{\text{p}}=r_{\text{p}}\cos\theta_{\text{p}}-D-r_h\cos\theta_h, \tag{33}$$

where D is referred to Figure 5 and given by

$$D=\frac{H\sin(\beta-\beta')}{\sin\beta\sin\beta'}. \tag{34}$$

Combining eqs. (33) and (34) yields the value of θ_{p}, for a given value of X_{p}.

Therefore, equating the internal energy dissipation rate to the external work rate, the stabilizing force F_{p} can be obtained as:

$$\begin{aligned} F_{\text{p}}=&\frac{1}{r_0\exp\left[(\theta_{\text{p}}-\theta_0)\tan\varphi\right]\sin\theta_{\text{p}}-mh}\\ &\left[K_c\gamma r_0^3(f_5-f_6-f_7-f_8)-cr_0^2f\right.\\ &\left.+pr_0^2(f_{\text{v}}+xKf_{\text{h}})+\gamma r_0^3(f_1-f_2-f_3-f_4)\right]. \end{aligned} \tag{35}$$

When the slope is at the instant failure state, the stabilizing force F_{p} reaches its maximum value, namely

$$F_{\text{pmax}}=\max\left\{F_{\text{p}}(\theta_0,\theta_h,\beta')\;\middle|\;\theta_{\text{p}}=f(X_{\text{p}})\right\}. \tag{36}$$

This can be solved with the optimization method.

The optimal location of piles can be determined when the stabilizing force provided by piles reaches the minimum value as the pile location changes between the toe and the crest of slopes. When both the optimal location and the stabilizing force of the piles are determined, the stabilizing piles used to prevent slope failure can be designed economically based on the corresponding design procedure.

4.2 Example

As shown in Table 2, the yield seismic acceleration factor of a slope (with β=45° and x=0.5) is 0.671. This is considered inadequate. Therefore, piles are used to increase the seismic acceleration factor to the desired value, for instance, 0.8 in this example. To facilitate the analysis, the dimensionless stabilizing force as $F=F_{\text{p}}/(\gamma H^2/2)$ [1] and the relative location as $\zeta=X_{\text{p}}/(H\cot\beta)$ are defined.

Figure 6 shows the increasing dimensionless stabilizing force with the decrease of anisotropic coefficient for homogenous and nonhomogeneous slopes. The dimensionless stabilizing force of the nonhomogeneous slope is much larger than that of homogenous slope. However, the increase rate of the homogeneous slope is larger than that of nonhomogeneous one. These phenomena illustrate that the anisotropy and nonhomogeneity of soils have significant effects on the stabilizing force required from piles to meet a pre-defined level of stability. Hence, if the anisotropic and nonhomogeneous properties of soils are neglected, the stabilizing force required from piles will be largely underestimated and the stabilized slope may still suffer from an expected earthquake.

The stabilizing force required from piles at different locations is also explored. As shown in Figure 7, the stabilizing force considering both anisotropy and nonhomogeneity of the soil is much larger than that only considering anisotropy or ignoring both. More importantly, the dimensionless stabilizing force increases with the increase of the relative location of piles. The closer to the crest of the slope is, the larger of the dimensionless stabilizing force is required. The dimensionless stabilizing force reaches its minimum value when the piles are placed near the toe of the slope. In another word, the optimal location for piles to reinforce the slope is near the toe

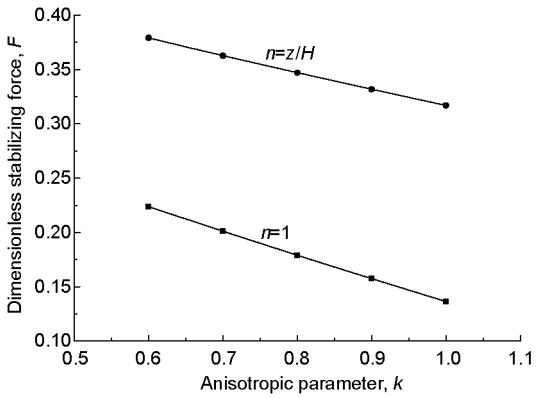

Figure 6 Effect of anisotropy and nonhomogeneity on dimensionless stabilizing force when relative location ζ=0.2.

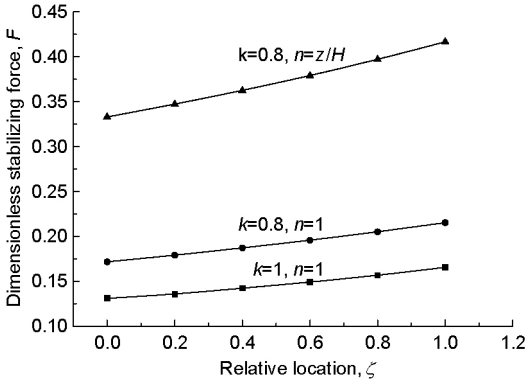

Figure 7 Effect of pile location on dimensionless stabilizing force.

of slope. Similar results have also been obtained by Ausilio et al. [1] and Nian et al. [3], but the effect of seismic loads on slope stability has not been incorporated in their studies.

5 Conclusions

The limit analysis method was employed to evaluate the seismic stability of anisotropic and nonhomogeneous slopes. The procedure was verified with the published studies for isotropic and homogeneous slopes. The results show that the anisotropy and nonhomogeneity of the soil greatly affect the magnitude of the yield seismic acceleration factor; the increase of the anisotropic coefficient reduces the yield seismic acceleration factor.

The study demonstrates that installing anti-slide piles is an effective means to stabilize slopes subjected to seismic loads by increasing the yield seismic acceleration factor to the desired level. Anisotropy and nonhomogeneity of the soil have significant effects on the stabilizing force required from the anti-slide pile. The larger the anisotropic coefficient is, the larger the stabilizing force the anti-slide pile needs to provide. In addition, the results show that the optimal location of the pile is near the toe of the slope, where the required stabilizing force is minimal for raising the yield seismic acceleration factor to a sufficient level.

This work was supported by the National Natural Science Foundation of China (Grant No. 41272288).

1 Ausilio E, Conte E, Dente G. Stability analysis of slopes reinforced with piles. Comp Geotechnics, 2001, 28: 591–611
2 Hassiotis S, Chameau J L, Gunaratne M. Design method for stabilization of slopes with Piles. J Geotechnical Geotech Geoenviron Eng, 1997, 123: 314–323
3 Nian T K, Chen G Q, Luan M T, et al. Limit analysis of the stability of slopes reinforced with piles against landslide in nonhomogeneous and anisotropic soils. Can Geotech J, 2008, 45: 1092–1103
4 Zhang G, Wang L. Stability analysis of strain-softening slope reinforced with stabilizing piles. J Geotech Geoenviron Eng, 2010, 136: 1578–1582
5 Zhang G, Wang L. Integrated analysis of a coupled mechanism for the failure processes of pile-reinforced slopes. Acta Geotech, 2016, 11: 941–952
6 Wu J, Cheng Q, Liang X, et al. Stability analysis of a high loess slope reinforced by the combination system of soil nails and stabilization piles. Front Struct Civ Eng, 2014, 8: 252–259
7 Li L, Li J, Sun D. Anisotropically elasto-plastic solution to undrained cylindrical cavity expansion in K0-consolidated clay. Comp Geotechnics, 2016, 73: 83–90
8 Zhou H, Liu H, Kong G, et al. Analytical solution of undrained cylindrical cavity expansion in saturated soil under anisotropic initial stress. Comp Geotechnics, 2014, 55: 232–239
9 Al-Karni A A, Al-Shamrani M A. Study of the effect of soil anisotropy on slope stability using method of slices. Comp Geotechnics, 2000, 26: 83–103
10 Chen W F. Limit Analysis and Soil Plasticity. Amsterdam: Elsevier Scientific Publishing Co., 1975
11 Donald I B, Chen Z. Slope stability analysis by the upper bound approach: Fundamentals and methods. Can Geotech J, 1997, 34: 853–862
12 Zhao L, Yang F, Zhang Y, et al. Effects of shear strength reduction strategies on safety factor of homogeneous slope based on a general nonlinear failure criterion. Comp Geotechnics, 2015, 63: 215–228
13 Tang G, Zhao L, Li L, et al. Stability charts of slopes under typical conditions developed by upper bound limit analysis. Comp Geotechnics, 2015, 65: 233–240
14 Yang X L, Xu J. Three-dimensional stability of two-stage slope in inhomogeneous soils. Int J Geomech, 2017, 17: 06016045
15 Xu J, Yang X. Effects of seismic force and pore water pressure on three dimensional slope stability in nonhomogeneous and anisotropic soil. KSCE J Civ Eng, 2017, 129
16 Chang C J, Chen W F, Yao J T P. Seismic displacements in slopes by limit analysis. J Geotechnical Eng, 1984, 110: 860–874
17 Chen W F, Chang C J, Yao J T P. Limit analysis of earthquake-induced slope failure. In: Proceedings of 15th Annual Meeting of the Society of Engineering Science. Gainesville, 1978. 533–538
18 Bray J D, Travasarou T. Pseudostatic coefficient for use in simplified seismic slope stability evaluation. J Geotech Geoenviron Eng, 2009, 135: 1336–1340
19 Nadukuru S S, Michalowski R L. Three-dimensional displacement analysis of slopes subjected to seismic loads. Can Geotech J, 2013, 50: 650–661
20 Pan Q, Dias D. Face stability analysis for a shield-driven tunnel in anisotropic and nonhomogeneous soils by the kinematical approach. Int J Geomech, 2016, 16: 04015076